

Electrophoretic Deposition of ^{10}B Nano/Micro Particles in Deep Silicon Trenches for the Fabrication of Solid State Thermal Neutron Detectors

Machhindra Koirala¹, Jia Woei Wu¹, Adam Weltz², Rajendra Dahal¹, Yaron Danon², and Ishwara Bhat^{1*}

¹Department of Electrical, Computer, and Systems Engineering,
Rensselaer Polytechnic Institute, Troy, NY, 12180, USA
*bhati@rpi.edu

²Department of Mechanical, Aerospace, and Nuclear Engineering,
Rensselaer Polytechnic Institute, Troy, NY, 12180, USA

Received 5 April 2017

Accepted 8 May 2018

We present a cost effective and scalable approach to fabricate solid state thermal neutron detectors. Electrophoretic deposition technique is used to fill deep silicon trenches with ^{10}B nanoparticles instead of conventional chemical vapor deposition process. Deep silicon trenches with width of 5-6 μm and depth of 60-65 μm were fabricated in a p-type Si (110) wafer using wet chemical etching method instead of DRIE method. These silicon trenches were converted into continuous p-n junction by the standard phosphorus diffusion process. ^{10}B micro/nano particle suspension in ethyl alcohol was used for electrophoretic deposition of particles in deep trenches and iodine was used to change the zeta potential of the particles. The measured effective boron nanoparticles density inside the trenches was estimated to be 0.7 gm cm^{-3} . Under the self-biased condition, the fabricated device showed the intrinsic thermal neutron detection efficiency of 20.9% for a $2.5 \times 2.5 \text{ mm}^2$ device area.

Keywords: Neutron detectors; electrophoretic deposition; silicon deep trenches; anisotropic etching.

1. Introduction

Solid state thermal neutron detector devices are pursued as possible replacement for He-based detectors because these detectors minimize many disadvantages of He-based detectors such as device bulkiness, high voltage requirement *etc.* [1-2]. Silicon devices themselves do not interact with thermal neutrons and hence a converter material such as LiF, ^{10}B , ^{157}Gd *etc.* has to be incorporated. These converter materials produce daughter particles that are charged and can be detected by corresponding silicon device [3-4]. A typical device involves fabrication of silicon pn junction and coating it by a thin boron. To get high efficiency, microstructured silicon pn junction devices are being used. This involves filling of silicon microstructure with ^{10}B [5] and the alpha particles produced during the interaction between thermal neutron and ^{10}B can reach to p-n junction. These

*Corresponding author.

alpha particles create electron-hole pairs in p-n junction. The electrons and holes are separated by the junction built-in potential and can be detected as an electrical signal. To optimize the neutron detection efficiency, the interaction of neutron with ^{10}B and charge collection by nearby p-n junction has to be optimized at the same time. To carry out such optimization, many micro-structured silicon devices have been proposed such as honeycomb structures, pillar structures, silicon trenches structures [6-8]. Among these microstructured silicon p-n junction for thermal neutron detection, honeycomb and pillar structures were fabricated by using deep reactive ion etching (DRIE) method [9] and have been reported previously.

DRIE method is expensive and may not be suitable for cost effective mass production. To overcome this situation, we proposed to modify the device fabrication method by replacing DRIE method by wet chemical etching method. Trenched silicon structure can be fabricated using anisotropic wet chemical etching of (110) silicon wafers following the technique developed in 1960's [10-11]. Previously, we have used low pressure chemical vapor deposition method (LPCVD) to fill the deep holes in silicon p-n junction to fabricate devices. However, for a trench structure, LPCVD deposition of boron film encounters many problems. One of the main problems is the stress introduced by the boron filling process. To overcome this stress problem caused by LPCVD, the filling of boron using nanoparticles was proposed. However, the nanoparticle filling results in less dense boron and this necessitates deeper trenches and thicker trench width. So, we explored electrophoretic deposition method for filling boron nano/micro particles in high aspect ratio silicon trenches and this paper addresses some results on the boron filling of trenches using boron nanoparticles. Device results on p-type silicon wafer and the results so obtained are also presented here for the first time.

Electrophoretic deposition is a colloidal processing technique in which thin film can be coated in a structured surface. The deposition process relies on the surface charge of the particles in a certain dispersive medium which determines the corresponding potential in its vicinity which introduces repulsive interaction among the particles. This potential is measured in terms of zeta potential which is defined as the potential at the share plane of the particle [12]. The dispersion medium having the absolute value of zeta potential higher than 30 mV is considered as a stable dispersion [13]. The zeta potential determines the rate of diffusion of a charged particle in the medium in an applied DC electric field. The absolute value of the zeta potential can be changed by changing the pH value of the dispersion medium. Addition of surfactant changes the charge balance condition and hence changes the zeta potential of the system. For example, the zeta potential of the particle in certain medium can be changed by adding iodine. Iodine produces H^+ ion in some organic solvents and changes the pH value of the liquid [14].

It has been reported that the electrophoretic deposition can be used to deposit thin film on to a structured surface with different spatial deposition selectivity. Generally, the patterning of the electrodes for electrophoretic deposition is done to control the materials deposition area and particles assembly [16]. Nadal *et al.*, have successfully demonstrated that the dielectric strip on the electrode can change the hydrodynamic flow of the

electrolyte solution [17] and colloidal particles can be deposited in a featured surface. In a similar fashion, Zhang *et al.*, have demonstrated the driving of CdSe nanoparticles in a template with nanoscopic features [18]. The method of electrophoretic deposition in a featured surface can be easily implemented to drive the boron nanoparticles in deep trenches using the parallel plate electrode model.

The modification of boron filling method is favorable from the device fabrication prospective as well. One of the key problems with our previous version of solid state thermal neutron detector was that after filling the trenches with LPCVD boron, a window opening is required to make front contact. To open an ohmic contact window in a honeycomb structure, dry etching of boron was done using SF₆ gas. Due to poor selectivity between boron and silicon etching, there is always the risk of top layer of silicon getting etched through the p-n junction and the device getting shorted. Using electrophoretic deposition technique, the silicon trenches can be filled at room temperature and the contact metallization on the device can be made even before boron nanoparticles filling. The boron nanoparticles at the contact surface can be simply wiped off after the deposition to make the contact.

This paper reports for the first time on the fabrication of the neutron detector in a p-type silicon wafer with boron filling carried out by the electrophoretic deposition process. The reason behind choosing a p-type wafer is that the p-region will be bulk of the wafer that absorbs the alpha particles generated by the boron converter material. Since the minority carriers are electrons, higher collection efficiency is possible since they have larger diffusion length compared to holes; they can travel much faster and can be collected by the thicker p-type region. In fact, in the silicon photovoltaic industry, 84% of the solar cells use p-type wafer as the absorber layer.

2. Experimental Procedure

2.1. Fabrication of silicon trenches

The schematic diagram of the fabricated device is presented in Fig. 1. A p-type (110) wafer with carrier concentration of $\sim 2 \times 10^{15} \text{ cm}^{-3}$ is used as a starting wafer. Front side of the wafer is doped n-type by diffusing phosphorous. The diffusion is done at 875 °C for 10 minutes using POCl₃ as pre-dep followed by diffusion for 40 minutes. The phosphosilicate glass grown during phosphorous diffusion was etched away using buffered oxide etch (BOE) solution. Device isolations were done using the dry etching of silicon using SF₆ in oxygen plasma which separates the dies with unit area of 2.5 mm x 2.5 mm. The exposed mesa side walls were passivated using 1.5 μm silicon dioxide. On the device area, silicon dioxide of thickness of 300 nm was deposited using plasma enhanced chemical vapor deposition (PECVD) method and the mask for trench etching was made using photolithography followed by plasma etching of oxide by CHF₃ gas in oxygen plasma. High aspect ratio silicon trenches were made using wet etching of silicon using TMAH at 100 °C for 40 minutes. From the wet etching of silicon, we obtained the silicon trenches with width of 5-6 μm and depth of 60-65 μm. The side wall of the silicon trenches is

2-3 μm . After trench etching, the sample was RCA cleaned and a continuous p-n junction was made using POCl_3 diffusion at 825°C with 10 minutes pre-dep and 30 minutes to diffuse phosphorus. The back side of the wafer is coated with Al using sputtering and the Al coated wafer is annealed at 400°C for 2 minute using rapid thermal annealing (RTA). After the fabrication of the sample, the trenches were filled by enriched boron nanoparticles using electrophoretic deposition process.

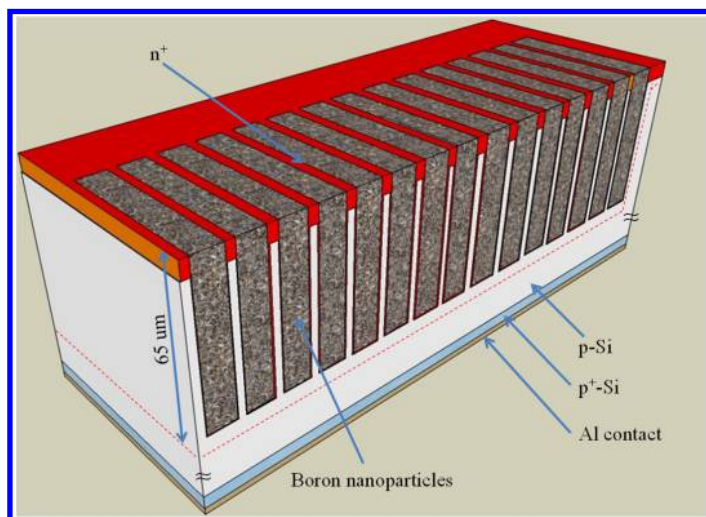


Fig. 1. Schematic cross-section of silicon trenched thermal neutron detector.

2.2. Analysis of enriched boron micro/nano particle suspension

The trenches are filled by boron using suspension of boron nanoparticles in ethyl alcohol. We have analyzed the surface charge behavior of ^{10}B micro/nano particles in ethyl solution. To enhance the surface charge density, we have used iodine as a surfactant. We prepared 3 different sets of boron nanoparticles. For the first one, we had used 0.1 mg of boron nanoparticles in 20 ml of ethyl alcohol. In the second suspension, 4 mg of iodine was dissolved in 20 ml of ethyl alcohol and 0.1 mg of boron nanoparticles was added. In the third suspension, 8 mg of iodine was dissolved in ethyl alcohol and 0.1 mg of boron nanoparticles was added. All of these three suspensions were sonicated separately and the zeta potential of these suspensions were measured using Zetasizer (Nicom-PSS). The results of the zeta potential measurement are presented in Fig. 2. The zeta potential increased from 6 mV without iodine to 11 mV with the addition of 8 mg of iodine. Hence, for boron micro/nano particles, the zeta potential, which controls the electrophoretic deposition rate can be changed using iodine as a surfactant.

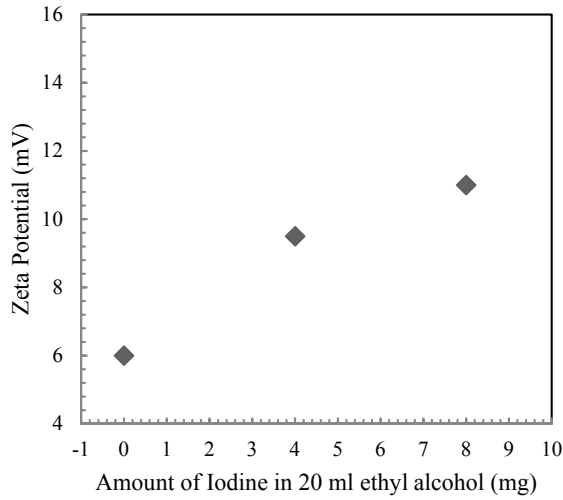


Fig. 2. Zeta potential of boron (^{10}B) micro/nano particle in ethyl alcohol with added iodine as a surfactant.

2.3. Silicon trench filling

To make the dispersion system for electrophoretic deposition, 40 mg of iodine was added and dissolved in 100 ml of ethyl alcohol (similar to adding 8 mg of iodine in 20 ml ethyl alcohol for the zeta potential measured suspension). Then, 1 gm boron nanoparticles were added to that ethyl alcohol and ultra-sonicated for 10 minutes. The schematic diagram for the electrophoretic deposition is shown in Fig. 3. As shown in the figure, silicon device is

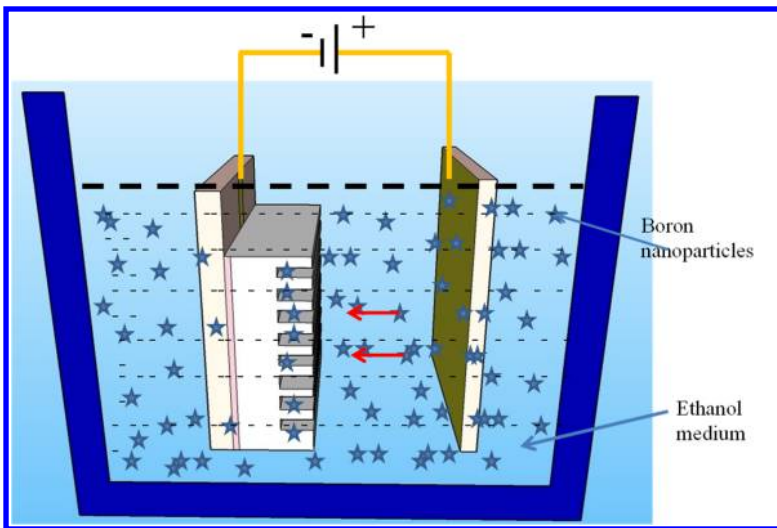


Fig. 3. Schematic diagram of experimental set up for electrophoretic deposition used for filling enriched boron micro/nano particles in silicon trenches.

attached in the cathode side. In this experimental configuration, the trajectory of the ^{10}B particles is perpendicular to the plate and is parallel towards the depth of the trench. After the device filling, the top part of the sample was wiped out to clean any over deposition. One part of the sample is cleaved and scanning electron microscope (SEM) image was taken. For the other piece of the sample, sputter coating of Ti/Al was done on the front part of the sample to make metallic contact. The sample was wire bonded using silver epoxy and I-V, C-V characterization and neutron detection efficiency was measured.

3. Results and Discussions

In this section, we will discuss the device characterization involving boron nanoparticles filling, electronic properties of the fabricated device and the device efficiency for neutron detection.

3.1. Boron nano/micro particles filling fraction

By weighing the silicon sample before and after nanoparticles filling, we could estimate the density of the filled nanoparticles. The volume of the trench is estimated by using pitch of the trench devices, width of silicon wall, width of trenches, and the depth of the trenches. The filling density of nanoparticles inside the trench was estimated to be 0.70 gm cm^{-3} .

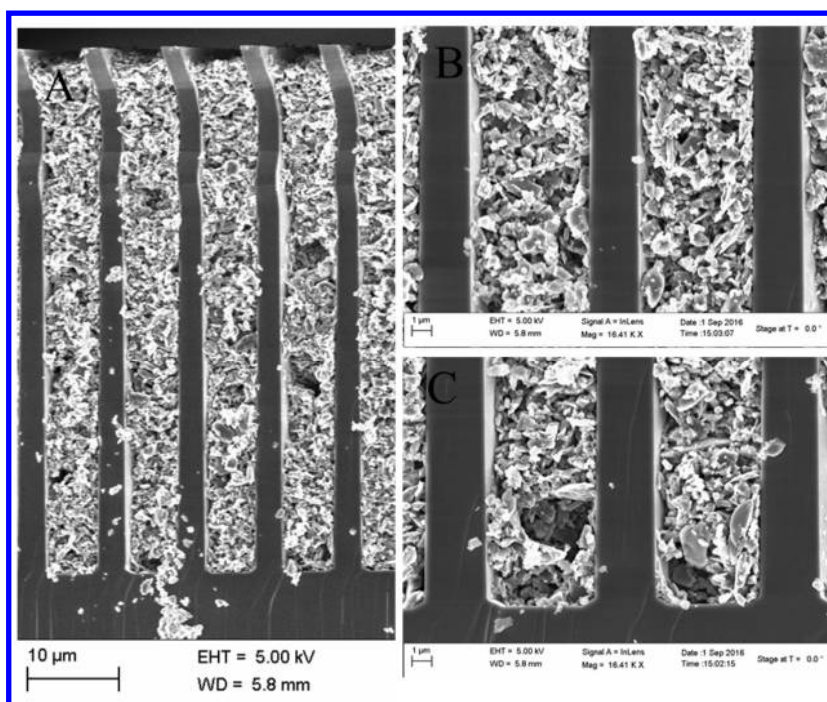


Fig. 4. SEM image of the cross-section ^{10}B filled silicon trenches. (A) SEM image of the filled sample. (B) Top part of the filled trench device. (C) Bottom part of the filled trench devices.

We obtained lower density for the nanoparticle filled trench devices compared to our previous LPCVD boron filled devices [19] which was 1.8 gm cm^{-3} . However, the depth of the holes in honeycomb structure were $45 \text{ }\mu\text{m}$ while the depth of the silicon trenches is $60 \text{ }\mu\text{m}$ giving larger space to fill boron. After boron nanoparticles were filled using electrophoretic deposition, the sample was cleaved and the images of the filled trench were taken using scanning electron microscope (SEM, SUPRA). The SEM images of the cross-section of samples are presented in Fig. 4. From the SEM images, we have seen that the micr/nano particles were filled up to the bottom of the trenches.

3.2. Leakage Current

Leakage current of the fabricated neutron detector p-n junction is important since it indicates the noise level of the detector. The leakage current was measured and the results are presented in Fig. 5. While calculating the device current density, we considered the top area of the device as the device active area which is 0.0625 cm^2 for a $2.5 \times 2.5 \text{ mm}^2$ die. In fact, this is not the true surface area of the p-n junction because of the trench profile of the device. The wall of the device is continuous p-n junction which has estimated surface area of the silicon wall is of the order of 0.72 cm^2 , so the effective leakage current density is one order of magnitude less than the reported value. Compared to our previous detector, the leakage current density in this device is high [15].

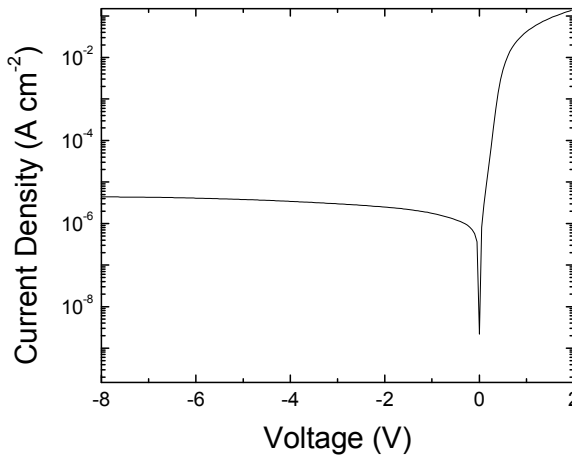


Fig. 5. I-V properties of $2.5 \text{ mm} \times 2.5 \text{ mm}$ silicon neutron detector.

3.3. Capacitance

One of the key parameters that affects the performance of neutron detector is the capacitance of the device. If the capacitance of the sample is high, the detection limit of the device goes down. Figure 6 shows the capacitance as a function of reverse biased voltage. The capacitance of $2.5 \times 2.5 \text{ mm}^2$ device at 0 V is 7 nF which sharply decreases

to 1 nF at 1V reverse biased voltage. To understand the capacitance behavior, we fabricated and measured the capacitance for a planner device of the same wafer and estimate the carrier concentration using Mott-Schottky relation as shown in Eq. (1).

$$\frac{1}{C^2} = \frac{2}{q\epsilon_{si}} \frac{1}{N_d} (V_0 + V_R) \tag{1}$$

where C is the capacitance per unit area, q is electronic charge, ϵ_{si} is permeability of silicon, N_d is the doping concentration of the wafer, V_0 is the barrier potential of silicon and V_R is the reversed biased voltage.

From Eq. (1), the carrier concentration of the wafer is calculated to be $1.7 \times 10^{15} \text{ cm}^{-3}$. Using the calculated carrier concentration, the depletion width of the p-n junction is estimated to be 750 nm. The thickness of the trench walls are 2-3 μm which is more than double of the depletion width. Because of the wider trench width, the devices are not fully depleted and the side wall of the trenches also contributes to capacitance. From the geometrical structure of the trenches, the surface area of the trenches is 0.72 cm^2 which is much higher compared to the planner area of the device which is 0.0625 cm^2 . For the undepleted condition, the effective area of the capacitor becomes 0.72 cm^2 while for the fully-depleting-condition the effective area of the capacitor become 0.0625 cm^2 . This is the main reason why the capacitance of the device is very high compared to planner diode of same area at zero biased condition. Using the reverse biased condition, we have calculated the capacitance for these two device areas and the results along with the measured capacitance data are presented in Fig. 6. From the capacitance plot, we can see that, a reversed biased voltage of 1 V is required for the device to get fully-depleted

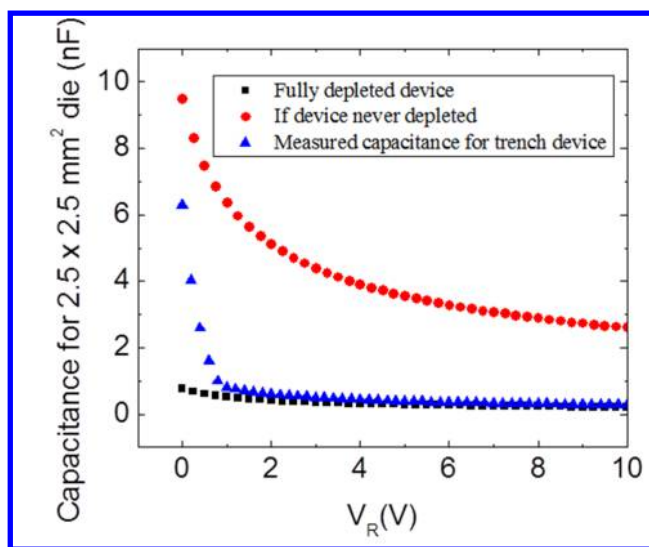


Fig. 6. Capacitance measured at different reverse biased voltage measured at 100 KHz. The capacitance has been calculated using the trenched structure with fully depletion and without depletion condition.

condition. From the capacitance point of view, there are couple of ways to improve the device to reduce the noise, one of them is to make the thinner trench with thickness less than $1.5\ \mu\text{m}$ (twice of the depletion width). Since, the wall with thinner width will be fragile and will be very hard for further processing such as nanoparticles filling, another way to improve the device performance is to use higher resistivity wafer. In such case the depletion width of the p-n junction will be larger and the fully depleted trenches can be obtained.

3.4. Neutron Counts

The efficiency of thermal neutron detector was done using calibrated fission neutron source of ^{252}Cf which is moderated by high density polyethylene housing of $61 \times 61 \times 40\ \text{cm}^3$. The neutron flux is calibrated and found that it has the flux of $298\ \text{n cm}^{-2}\ \text{s}$ at the distance of 8 cm from the source. We measured the neutron count for our devices at different conditions (i) at the lead housing when there is no neutron source in the room, (ii) at 8 cm away from the neutron source, (iii) with 2 mm thick Cd sheet in between neutron source and the detector, and (iv) with ^{60}Co source to measure the gamma response. The result of the neutron response measurement is presented in Fig. 7. When there is no source and the device is in the lead brick housing, the device has the noise level of 600 KeV. Then the device is measured using ^{252}Cf source which gives the count for thermal as well as fast neutron. Later, a Cd shielding of 2 mm width has been used to shield the thermal neutron and only high energy neutrons were detected. We subtracted the high energy neutron counts to obtain the thermal neutron counts. We obtained the thermal neutron counts of

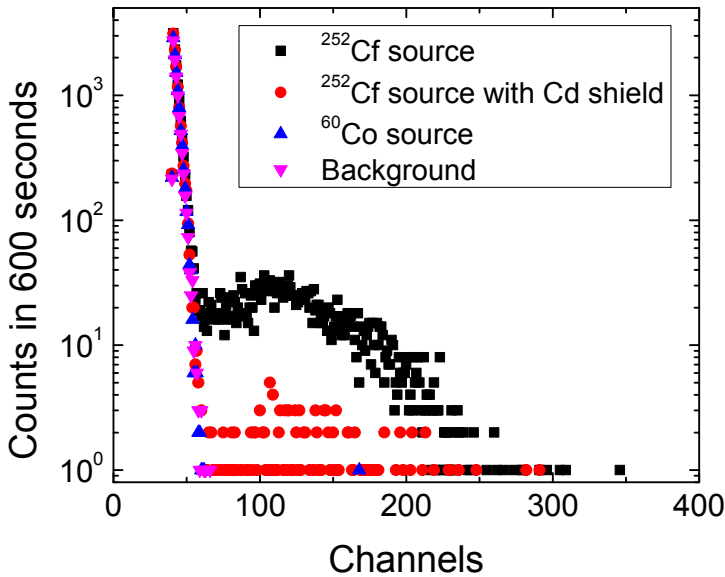


Fig. 7. Pulsed height spectrum for the trench structured neutron detector filled with boron micro/nano particles.

2333 in 600 seconds for the incoming neutron flux of $298 \text{ n cm}^{-2} \text{ s}$. Figure 7 shows the count rate of thermal neutrons at different energy ranges. From the data, we have found the detection efficiency of our device is to be 20.9%.

4. Detector Cost Reduction

Mass production is needed to diversify the use of solid state neutron detector over the ^3He gas based neutron detector. To reduce cost, our ^{10}B filled silicon trench based thermal neutron detectors is a viable alternative. We made key changes in the device processing methodology to reduce the device cost. One of the methods used in our detector is the wet chemistry method for trench etching and is an easy technique compared to DRIE method for making silicon trenches. The use of electrophoretic deposition method is also a cost effective method over LPCVD. The low pressure CVD method involves the use of expensive enriched diborane gas. The filling using electrophoretic deposition can use boron nanoparticles and that can be done by using some home-made customized tools.

5. Conclusions

In conclusion, we have implemented the wet etching method for trench etching and electrophoretic deposition for filling the silicon trenches by ^{10}B nanoparticles. The loosely filled nanoparticles has the density of 0.7 gm cm^{-3} in silicon trenches of 5-6 μm width and 60-65 μm depth. We have successfully demonstrated that the EPD filling method can fill to the bottom of the high aspect ratio silicon trenches. Following the process mentioned earlier, we obtained the neutron detection efficiency of 20.9% for solid state thermal neutron detectors. This is the first publication of neutron detector fabrication in p-type silicon using electrophoretic deposition process for boron filling.

Acknowledgement

The authors would like to thank the support staff of the Rensselaer Polytechnic Institute Micro-Nano-Clean-Room. This work was financially supported by USDHS/DNDO under grand number ECCS-1348269 and 2013-DN-077-ER0001.

References

1. GAO (U. S. Government Accountability Office), *Technology assessment: Neutron detectors: alternatives to using Helium-3*, 2011, GAO-11-753.
2. J. F. C. A. Veloso, F. D. Amaro, J. M. F. dos Santos, J. A. Mir, G. E. Derbyshire, R. Stephenson, N. J. Rhodes and E. M. Schooneveld, Application of the microhole and strip plate detector for neutron detection, *IEEE Transaction on Nuclear Science*, **51**, 2104 (2004).
3. D. S. McGregor, M. D. Hammig, Y.-H. Yang, H. K. Gersch, R. T. Klann, Design consideration for thin film coated semiconductor thermal neutron detectors-I: basics regarding alpha particles emitting neutron reactive films, *Nucl. Instrum. Methods Phys. Res. A*, **500**, 272 (2002).
4. D. S. McGregor, W. J. McNeil, S. L. Bellinger, T. C. Unruh, J. K. Shultis, Microstructured semiconductor neutron detectors, *Nucl. Instrum. Methods Phys. Res. A*, **608**, 125 (2009).

5. F. Sarubbi, T. L. M. Scholtes, L. K. Nanver, Chemical vapor deposition of alpha-boron layers on silicon for controlled nanometer-deep p⁺n junction formation, *J. Electron Mater.* **39**, 162 (2010).
6. N. LiCause, J. Dingley, Y. Danon, J.-Q. Lu, I. B. Bhat, A novel solid-state self-powered neutron detector, *Proc. of SPIE-7079*, 707908 (2008).
7. R. J. Nikolic, Q. Shao, L. F. Voss, A. M. Conway, R. Radev, T. F. Want, M. Dar, N. Deo, C. L. Cheung, L. Fabris, C. L. Britton and M. N. Ericson, Si pillar structured thermal neutron detectors: fabrication challenges and performance expectations, *Proc. of SPIE-8031*, 803109 (2011)
8. K.-C. Huang, R. Dahal, J. J.-Q. Lu, A. Weltz, Y. Danon, I. B. Bhat, Scalable large-area solid-state neutron detector with continuous p-n junction and extremely low leakage current, *Nucl. Instrum. Methods Phys. Res. A*, **763**, 260 (2014).
9. K. C. Hunag, R. Dahal, J. J.-Q. Lu, Y. Danon, I. B. Bhat, Boron filling of deep holes for solid-state neutron detector applications, *Transaction of American Society*, **106**, 105 (2012).
10. J. M. Crishal and A. O. Harrington, *Electrochem. Soc. Extended Abstract*, Los Angeles, CA, 1962, Abs. No 89.
11. D. B. Lee, Anisotropic etching of silicon, *J. Appl. Phys.*, **40**, 4569 (1969).
12. L. Bousse, S. Mostarshed, B. V. D. Shoot, N. F. de Rooij, P. Gimmel, W. Gopel, Zeta potential measurement of Ta₂O₅ and SiO₂ thin films, *J. Colloid Interface Sci.*, **147**, 22 (1991).
13. J. D. Clogston, A. K. Patri, Zeta potential measurement, *Methods Mol. Biol.*, **697**, 63 (2011).
14. L. Dusoulier, R. Cloots, B. Vertruyen, R. Moreno, O. Burgos-Montes, B. Ferrari, YBa₂Cu₃O_{7-x} dispersion in iodine acetone for electrophoretic deposition: Surface charging mechanism in a halogenated organic media, *J. Eur. Ceram. Soc.*, **31**, 1075 (2011).
15. R. C. Bailey, K. J. Stevenson, J. T. Hupp, Assembly of micropatterned colloidal gold thin film via microtransfer molding and electrophoretic deposition, *Advanced Materials*, **12**, 1930 (2000).
16. F. Qian, A. J. pascal, M. Bora, T. Y.-J. Han, S. Guo, S. S. Ly, M. A. Worsley, J. D. Kuntz, and T. Y. Olson, On-demand and local selective particle assembly via electrophoretic deposition for fabricating structure with particle-to-particle precision *Langmuir*, **31(12)**, 3563 (2015).
17. F. Nadal, F. Argoul, P. Kestener, B. Pouligny, C. Ybert, and A. Ajdari, Electrically induced flows in the vicinity of a dielectric stripe on a conducting plane, *Eur. Phys. J. E*, **9**, 387 (2002).
18. Q. Zhang, T. Xu, D. Butterfield, M. J. Misner, D. Y. Ryu, T. Emrick, and T. P. Russell, Controlled placement of CdSe nanoparticles in diblock copolymer template by electrophoretic deposition, *Nano Letts.*, **5(2)**, 357 (2005).
19. R. Dahal, K. C. Huang, J. Clinton, N. LiCausi, J.-Q. Lu, Y. Danon, I. B. Bhat, Self-powered micro-structured solid state neutron detector with very low leakage current and high efficiency, *Appl. Phys. Lett.*, **100**, 243507 (2012).